

# Identification of a Novel IL-6 Isoform Binding to the Endogenous IL-6 Receptor

Michel P. Bihl, Karl Heinemann, Jochen J. Rüdiger, Oliver Eickelberg, André P. Perruchoud, Michael Tamm, and Michael Roth

Pulmonary Cell Research and Human Genetics, Department of Research, Zentrum für Lehre und Forschung, Kantonsspital Basel, Basel, Switzerland; and Department of Pathology, University Hospital Yale, Yale University, New Haven, Connecticut

Interleukin (IL)-6 is a multifunctional cytokine showing a wide variety of biologic functions on various tissues. Extracellular IL-6 signals through heterohexameric complex formation with IL-6 receptor- $\alpha$  (IL-6R $\alpha$ ) and IL-6 receptor- $\beta$  (IL-6R $\beta$ ). In analogy to cytokines IL-2 and IL-4, we investigated the expression of IL-6 splice variants in lung tissue and cultivated fibroblasts. In human lung specimens, four different IL-6 transcripts were characterized as follows: native IL-6; IL-6 missing either exon 2 (IL-6 $\Delta$ 2), exon 4 (IL-6 $\Delta$ 4), or missing both; and exons 2 and 4 (IL-6 $\Delta$ 2,4). Only native IL-6 and IL-6 $\Delta$ 4 encoded for proteins of ~ 26 and 17 kD, respectively. Although the overall structure and most functional sites of the IL-6 $\Delta$ 4 protein were predicted to be maintained, IL-6 $\Delta$ 4 was found to lack two amino acids necessary for IL-6/IL-6 homodimerization as well as two of the six amino acids required for interaction with IL-6R $\beta$ . Receptor mobility shift assays confirmed that the new isoform formed a stable complex with IL-6R $\alpha$ ; however, no interaction with IL-6R $\beta$  was observed. Thus, IL-6 $\Delta$ 4 is likely to compete with native IL-6 for IL-6R $\alpha$  binding but fails to transmit IL-6R $\beta$ -mediated signaling.

Interleukin (IL)-6 is a multifunctional cytokine which regulates multiple cellular activities. IL-6 was reported to promote or restrain cell growth, or cell differentiation, in a cell type-specific manner (1). In particular, extracellular IL-6 has been implicated in the differentiation of B-cells, T cells, macrophages, and neuronal cells. Its role in growth promotion has been shown in various B-cells (2) and hematopoietic stem cells (3). Intracellular IL-6, on the other hand, appears to control proliferation in ectodermal cells such as keratinocytes (4) and melanoma cells (5, 6), as well as in mesenchymal cells including primary human lung fibroblasts (7), vascular smooth muscle cells, and mesangial cells (8). Importantly, IL-6 production seems to correlate with tumor progression in human cancer, such as pleural mesothelioma, glioblastoma, and ovarian and prostate carcinoma (9–12). This wide spectrum of activities can partially be explained by at least two different IL-6-inducible signaling pathways, one acting extracellularly, through the IL-6 receptor complex, and the other located intracellularly via a yet undefined pathway.

The diversity of extracellular IL-6 signaling reflects several possible combinations between IL-6 and its receptors, IL-6R $\alpha$ , and/or competition of other receptors with its signal transducer, IL-6R $\beta$ . IL-6R $\alpha$  exists in a membrane bound and a soluble form, generated either by shedding or alternative

splicing (13–15). Both isoforms of the IL-6 R $\alpha$  are capable of binding to the signal transducer IL-6R $\beta$ . Consequently, the soluble IL-6R $\alpha$  is able to transduce the signal to cells devoid of membrane-bound IL-6R $\alpha$ , but expressing IL-6R $\beta$  (16). IL-6R $\beta$  also serves as a transducing element for other cytokines (e.g., oncostatin M) and cytokine receptors (e.g., leukemia-inducible factor receptor, ciliary neurotrophic factor receptor) (17, 18).

Expression of IL-6 is regulated by nuclear factors, which modulate gene expression as activators, such as nuclear factor (NF)-IL-6 and NF- $\kappa$ B, or inhibitors, e.g., glucocorticoid receptor, and by members of the suppressor of cytokine-signaling family, such as SOCS-1 and SOCS-3 (19). Control of cell type-specific action of intra- and extracellular IL-6, however, can only partially be explained by differences in on/off gene expression. Other mechanisms like mRNA and protein maturation may thus be implicated in regulating an IL-6-specific response, as has been suggested by studies on the regulation of IL-2 and IL-4 (20–23). Both genes produce alternatively spliced transcripts encoding for proteins with antagonist (IL-4) or competitive antagonist (IL-2) properties.

To further elucidate the regulatory mechanisms of IL-6 in mesenchymal cells, we investigated the occurrence and expression of IL-6 transcripts in human lung tissue. Here, we report three new IL-6 mRNA isoforms, one of which yields a 17-kD protein. This new isoform binds to IL-6R $\alpha$  but lacks several binding sites required for IL-6/IL-6R $\alpha$  complex formation with IL-6R $\beta$ .

## Material and Methods

### Cell Culture

As described by Roth and coworkers, primary human lung fibroblast cells were established from sterile lung specimens, obtained from patients undergoing lobectomy or pneumonectomy for peripheral lung cancer as described previously (24). Fibroblasts were cultivated in RPMI 1640 medium supplemented with L-Glutamine (8 mM; Gibco BRL, Basel, Switzerland), 5% fetal calf serum (Fakola, Basel, Switzerland), and 20 mM HEPES (Fakola). IL-6 mRNA analysis was performed in subconfluent cell cultures (80%). All primary cultures of fibroblasts were used between passages 2 and 6. Primary human fibroblasts were transiently transfected with the IL-6-pd2EGFP construct and cultivated in the fibroblast medium described above. Human hepatoma HUH7 cells were stably transfected and cultivated in MEM-EARLE medium supplemented with 2.2 g/liter NaHCO<sub>3</sub>, 0.518 g/liter N-acetyl-L-alanyl-L-glutamine, G418 Sulfate 500  $\mu$ g/ml (Calbiochem, Lucerne, Switzerland), penicillin/streptomycin 100 U/100  $\mu$ g/ml (Seromed, Basel, Switzerland).

### mRNA Isolation and RT-PCR

IL-6 mRNA isoforms were isolated from cell cultures or healthy human lung tissue. Using a Polytron PT 1200 C/T (Kinematica

(Received in original form May 23, 2001 and in revised form March 21, 2002)

Address correspondence to: Michael Roth, Ph.D., Hebelstrasse 20, ZLF, University Hospital Basel, 4031 Basel, Switzerland. E-mail: michel.bihl@unibas.ch

Abbreviations: interleukin, IL; nuclear factor, NF.

Am. J. Respir. Cell Mol. Biol. Vol. 27, pp. 48–56, 2002  
Internet address: www.atsjournals.org

AG, Littau, Switzerland), 1 mg of tissue was homogenized in buffer RLT (Qiagen AG, Basel, Switzerland) and mRNA was extracted using the RNeasy kit according to the manufacturer's instructions (Qiagen). First-strand cDNA synthesis was performed from 600 ng total RNA in a total volume of 20  $\mu$ l using Superscript II following the standard protocol provided by the manufacturer (Gibco BRL, Basel, Switzerland). RT-PCR conditions involved an initial denaturation step at 94°C for 3 min, followed by 40 cycles with denaturation at 94°C for 15 s, annealing at 58°C for 20 s, and extension at 72°C for 60 s, followed by a final extension step at 72°C for 5 min. Ten microliters of each PCR reaction mixture were size-fractionated by electrophoresis on 2.0% agarose gels (NuSieve GTG; FMC BioProducts, Rockland, ME) in TBE-buffer (1  $\times$  TBE = 89 mM Tris base, 89 mM boric acid, 2 mM EDTA), and visualized by ethidium bromide staining under UV light.

Two different primer sets were used: One encompassing the complete *IL-6* coding sequence (IL-6 full 5': GCT CTA TCT CCC CTC CAG GAG and IL-6 full 3': ACC AGA AGA AGG AAT GCC CAT) and a second, starting 8 nt upstream of exon 1 (IL-6 ctrl 5': GCC CAG CTA TGA ACT CCT TCT C) and omitting the last 65 nt of exon 5 (IL-6 ctrl 3': GAG TTG TCA TGT CCT GCA GCC).

### IL-6 mRNAs Sequence Analysis

Each specific RT-PCR product band was isolated from agarose gel with a sharp scalpel. DNA was extracted from the band using a QIAEX II Agarose extraction kit (Qiagen) according to the QIAEX II agarose gel extraction protocol. DNA was eluted by 20  $\mu$ l of 10 mM Tris-Cl, pH 8.5, and 0.5  $\mu$ l was directly used for reamplification. Reamplification comprised 25 cycles with denaturation at 94°C for 15 s, annealing at 58°C for 20 s, and extension at 72°C for 60 s, followed by a final extension step at 72°C for 5 min. Direct cDNA sequencing of all *IL-6* isoforms was performed using a Thermo Sequenase cycle sequencing kit (Amersham Pharmacia, Dübendorf, Switzerland). The primers were end-labeled with an infrared dye, IRD-800, and used directly in the cycle sequencing reaction. Cycle sequencing parameters were 95° for 30 s, 55° for 30 s, 72° for 1 min, 25 times. Due to the short coding sequence of exon 1 (19 bp), both strands were sequenced to determine the proper 5' sequence for each isoform. Subsequently, the products were loaded on a 6% denaturing polyacrylamide gel and analyzed on a fluorescence-based automated DNA sequencer according to the manufacturer's instructions (LI-COR, Lincoln, NE).

### In Vitro Transcription/Translation of IL-6 cDNA Splice Variants

Four-microliter aliquots of each *IL-6* isoform served as template in an *in vitro* transcription and translation reaction applying the TNT T7 coupled reticulocyte lysate system according to the manufacturer's instructions (Catalys/Promega, Wallisellen, Switzerland). Briefly, 2  $\mu$ l of PCR product was added to 3  $\mu$ l of PTT-Mix (256  $\mu$ l of PTT-Mix contained the Promega product at following proportion: TNT RRL 200  $\mu$ l, RNasin 8  $\mu$ l, TNT reaction buffer 16  $\mu$ l, methionine-free amino acid mixture 8  $\mu$ l, and TNT polymerase 8  $\mu$ l). The products of the different *IL-6* splice variants were labeled by adding 0.5  $\mu$ l of <sup>35</sup>S methionine (1 mCi/ml) (Amersham Pharmacia) to each reaction. The *in vitro* translation was performed for 1 h at 30°C. Products were size-fractionated on a 12% SDS polyacrylamide gel for 35 mA/gel for 110 min, which subsequently was fixed (10% glacial acetic acid, 30% methanol) for 1 h, dried for 45 min at 80°C, and exposed to Biomax film (Kodak, Rochester, NY).

### Immunoprecipitation and Western Blot Analysis of IL-6 Isoforms

For *in vitro* analysis, human lung fibroblasts were grown to 60% confluence and incubated for 16 h in methionine-free RPMI 1640

(Seromed) in the presence of 100 mCi/ml of <sup>35</sup>S methionine (activity > 1,000 Ci/mmol; Amersham Pharmacia Biotech). Cell supernatant was used for detection of secreted IL-6 isoforms. Adherent cells were washed twice with phosphate-buffered saline before they were lysed in 100  $\mu$ l of lysate buffer (50 mM Tris-Cl [pH 8], 150 mM NaCl, 0.02% Na-azide, 100  $\mu$ g/ml PMSF, 1  $\mu$ g/ml aprotinin, 1% Triton X-100). Ten microliters of cell lysate or 100  $\mu$ l of cell supernatant were immunoprecipitated in 10 times the volume of NET-buffer (50 mM Tris [pH 7.5], 1 mM EDTA [pH 8], 150 mM NaCl, 0.02% Na-azide, 0.1% NP-40 and 0.25 gelatine, 0.1 mM PMSF), and the protease inhibitor cocktail Complete (Roche Diagnostic, Basel, Switzerland).

Probes were immunoprecipitated with goat anti-human IL-6 antibody (R&D, Oxon, UK), and immune complexes were recovered with protein G-Sepharose beads (Calbiochem) for 2 h at 4°C. Equal amounts of immunoprecipitated proteins were separated on SDS-PAGE gels and electroblotted to Immobilon membranes (Millipore). The ability of anti-human antibody to recognize both isoforms was verified using recombinant *in vitro* translated IL-6.

In a first step the membranes were exposed to a PhosphorImager cassette and <sup>35</sup>S-labeled proteins were visualized using a computer-assisted analyzing program (ImageQuant; Molecular Dynamics, Sunnyvale, CA). In a second step, the membranes were used for Western blot analysis using a polyclonal anti-human IL-6 antibody (final dilution 1:2,000; R&D) or mouse anti-human IL-6 antibody (1:1,000; R&D) for 2 h at room temperature. After three washes, membranes were exposed for 1 h (room temperature) to a secondary rabbit anti-goat horseradish peroxidase-conjugated antibody (1:10,000), and protein bands were visualized using the ECL system (Amersham Pharmacia).

For *in vivo* analysis of IL-6 protein isoforms, 5 g of freshly resected lung tissue were lysed in denaturing SDS lysis buffer (0.5% wt/vol SDS; 0.05 M Tris-Cl, pH 8; 1 mM DTT; and the protease inhibitor cocktail Complete [Roche]). The samples were sonicated (1 min) and centrifuged (13,000  $\times$  g, 10 min, 4°C) and supernatants were size-fractionated in a SDS gradient (4–15%) acrylamide gel. Western blot analyses were performed as described above.

Expression of IL-6-EGFP fusion protein. IL-6 isoforms were amplified using primers containing ApaI restriction site. Amplicons and pGEMT Easy vector (Promega) were digested with ApaI enzyme (Roche Diagnostics) for 1 h at 37°C. Ligation of 10 ng pGEMT Easy vector was performed in a total volume of 20  $\mu$ l using three different amounts of IL-6 isoform amplicon: 1.67, 5, and 16.7 ng (T4 DNA ligase; Promega). Five microliters of the ligation mix were used for the transformation of the JM109 cell line (Promega), according to manufacturer's instructions. Colonies of transfected bacteria were verified by sequence analysis (Microsynth, Balgach, Germany). Plasmid DNA was isolated from colonies containing IL-6 $\Delta$ 4 fragment. IL-6 isoform-pd2EGFP constructs were made using the following procedure: DNA of IL-6 $\Delta$ 4-pGEMT Easy and pd2EGFP (Clontech, Basel, Switzerland) were digested using ApaI restriction enzyme and DNA fragments were separated by agarose gel electrophoresis and extracted from the gel using a NucleoSpin Extract kit (Macherey-Nagel, Oesingen, Switzerland). Ligation into the pd2EGFP vector was performed in a total volume of 20  $\mu$ l using 50 ng of IL-6 $\Delta$ 4-ApaI and 10 ng of pd2EGFP-ApaI fragments (T4 DNA ligase; Promega). Forty microliters of JM109 competent cells were transfected with 5  $\mu$ l of ligation mix and plated in LB agar plates.

### Transfection of Primary Lung Fibroblasts and the Human HUH7 Cell Line

Cells were cultured to 80% confluence into six-well plates (Falcon, Basel, Switzerland) and transfected using Effectene kit (Qiagen) according to the instruction of manufacturer. Briefly, 1.6  $\mu$ l of

Enhancer was added to 0.2  $\mu\text{g}$  of the vector, adjusted to 60  $\mu\text{l}$ , and incubated at room temperature for 5 min. Two microliters of Effectene transfection reagent was added to the DNA-Enhancer mixture, mixed by pipetting up and down, and incubated at room temperature for 15 min. Cells were washed once with phosphate-buffered saline and plated in 1.6 ml of MEM-EARLE. A quantity of 350  $\mu\text{l}$  of culture medium was added to the vial containing the transfection complex, mixed, then added to each well of the six-well plate. IL-6-EGFP fusion protein expression in primary human lung fibroblasts was analyzed by confocal microscopy 48 h after the transfection. In experiments using HUH7 cells, after 18 h of cell culture, medium was replaced by MEM-EARLE medium containing 800  $\mu\text{g}/\text{ml}$  of G418 Sulfate. After 9 d of cell culture under antibiotic resistance conditions, stably transfected HUH7 cells were detected as growing colonies. Single colonies were selected and transferred into a single well of a six-well plate. Expression of EGFP-IL6 $\Delta$ 4 fusion protein was detected by confocal microscopy (Zeiss, Jena, Germany) using LSM510 software.

### Structural Comparison and Prediction

The three-dimensional structure of IL-6 $\Delta$ 4 was reconstructed in comparison to the NMR structure of the full-length IL-6 (25). Structures were aligned by performing a direct alignment of the AA sequences of IL-6 and IL-6 $\Delta$ 4 (Macaw 2.05), after which SwissPDB Viewer 3.51 (GlaxoSmithKline R&D, Geneva, Switzerland, www.expasy.ch) was used to edit three-dimensional structure information. Structure of full-length IL-6 was achieved from the Bookhaven Protein databank as PDB format (2IL6, an NMR structure of full-length IL-6). Because this file contains 32 slightly different structures of IL-6, we further used the original structure in that file. Protein sequence of the short IL-6 isoform resulted from the translation proposed according to the sequenced mRNA of IL-6 $\Delta$ 4. This revealed an identical AA sequence of both IL-6 isoforms except that IL-6 $\Delta$ 4 lacks AAs encoded by exon 4. Therefore, we decided to predict the structure of the new IL-6 $\Delta$ 4 according to the 2IL6 (PDB entry code)-NMR structure. At first, all exon 4-encoded AAs E82 to K130 of the 2IL6 PDB file were deleted. This resulted in a three-dimensional structure with the AA sequence of the IL-6 $\Delta$ 4, which consists of two unconnected AA chains, the first from L20 to E81 and the second from A131 to M185; the gap between the carboxy terminus at E81 and the amino terminus at A131 was measured to be 10.9 Å. Before aligning the backbone in that region, we slightly rotated the backbone bounds between L131 and P138 until the distance between the carboxy terminus of the first and the amino terminus of the second strand was less than 1.5 Å. To correct binding angles and atom distances we used the energy minimization tool (20 steps, steepest descent 3 times) for the AAs between F79 to P140.

### Receptor Mobility Shift

*In vitro* translated IL-6 $\Delta$ 4 protein was incubated for 20 min at room temperature in the presence or absence of IL-6R $\alpha$  and/or IL-6R $\beta$ . Complex formation between IL-6 $\Delta$ 4 and IL-6 receptors

was analyzed by electrophoresis on a 4–20% gradient gel (electrode buffer; 25 mM Tris-Base, 192 mM Glycine pH 8.8, non-denaturing sample buffer; 0.0625 M Tris-Cl, pH 6.8, 10% glycerol, and 0.01% bromophenol blue) and the proteins were blotted (40 mA/gel, 90 min, in a buffer containing 25 mM Tris/200 mM Glycine pH 8.2 and 10% methanol) on a PVDF membrane (Millipore, Bedford, MA). <sup>35</sup>S-methionine-labeled IL-6 $\Delta$ 4 was directly visualized on the PhosphorImager system (Molecular Dynamics). IL-6R $\alpha$  was detected using a polyclonal anti-IL-6R $\alpha$  antibody (R&D Systems) and visualized by chemiluminescence through addition of a rabbit anti-goat IgG horseradish peroxidase-coupled antibody using the ECL kit (Pierce, Rockford, IL).

## Results

### Detection of Different IL-6 Isoforms in Human Lung Tissue

The presence of IL-6 mRNA in lung tissue and primary human lung fibroblasts was investigated by RT-PCR. In addition to full-length IL-6 mRNA, we could distinguish four additional PCR bands (Figure 1A). The coamplification was verified using a second set of IL-6 primers. The band pattern obtained was identical for both amplifications when taking into account a length difference of 133 nt depending on the primer set used. The intensity of the various PCR bands differed considerably, with band 1 being the most intense, band 4 being of intermediate intensity, and bands 2, 3, and 5 of low intensity. Following extraction and reamplification of the respective PCR products, all but band 2 were reproduced (Figure 1B). Reamplification of band 2 resulted in a PCR product migrating at the same height as band 4. The specific size of the different PCR products strongly suggested the existence of alternatively spliced variants of IL-6 mRNA.

### Analysis of the Different IL-6 Isoforms

To determine their origin, the four reamplified cDNA products were analyzed by direct sequencing. As deduced from the respective fragment sizes, we found that each cDNA product represented an alternatively spliced isoform of IL-6 (Figure 2): band 1 corresponding to full-length IL-6 (715 bp); band 3 (568 bp) to IL-6 missing exon 2 (IL-6 $\Delta$ 2); band 4 (523 bp) to IL-6 missing exon 4 (IL-6 $\Delta$ 4); and band 5 (376 bp) representing IL-6 lacking exons 2 and 4 (IL-6 $\Delta$ 2,4).

In the case of the IL-6 $\Delta$ 2 and IL-6 $\Delta$ 2,4 isoforms, exon 2 is missing and exon 1 directly joins exon 3 at bp 19 and 211. This splicing of exon 2 results in the disruption of the reading frame. Thus, premature stop codons were generated yielding a truncated IL-6 peptide of eight amino acids

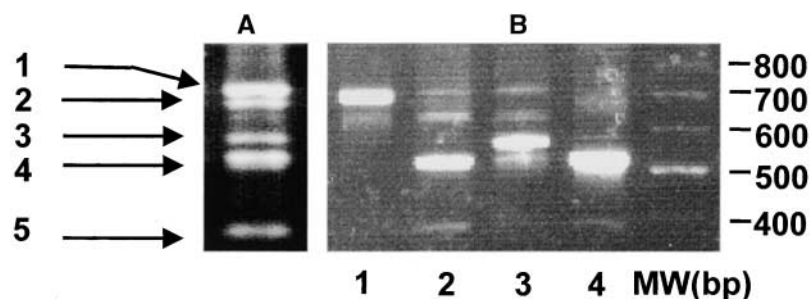
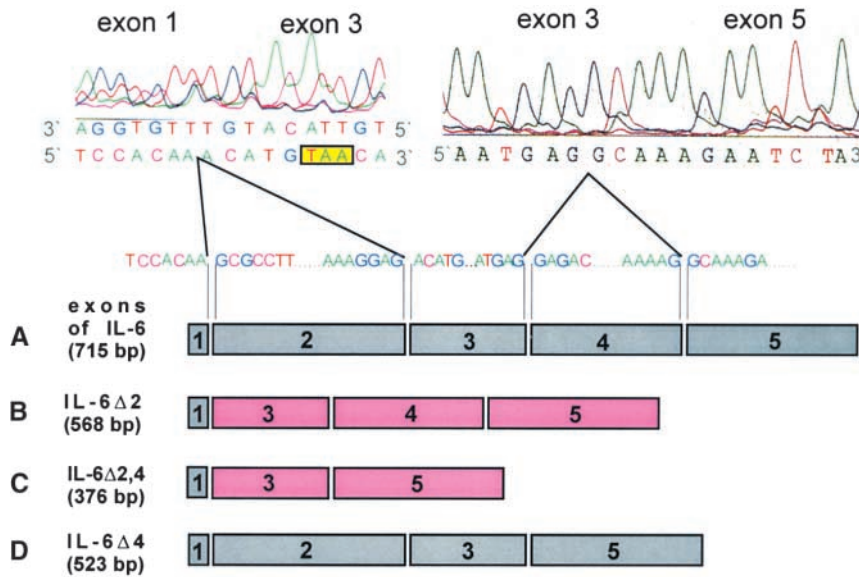


Figure 1. RT-PCR amplification pattern of total RNA extracted from human lung tissue. (A) IL-6-specific primers were used for coamplification of five cDNA products. The PCR-products from IL-6 mRNAs are numbered from 1 to 5. Products corresponding to bands 1 to 4 were isolated and reamplified (B), and cDNA fragments were visualized by ethidium bromide staining under UV light.



**Figure 2.** Sequence analysis of products obtained from IL-6-specific RT-PCR. The chromatograms in the upper part illustrate the splicing of exon 2 and exon 4. The first stop codon generated by splicing of exon 2 is represented by a yellow box. Splice variants keeping the reading frame are displayed in gray, whereas those losing it are colored in pink. PCR products described in Figure 1 were further characterized by sequence analysis as follows: (A) full-length IL-6; (B) IL-6 missing exon 2 (IL-6Δ2); (C) IL-6Δ2,4; and (D) to IL-6Δ4.

(Figure 2, yellow box). On the contrary, splicing of exon 4 did not alter the reading frame. *IL-6Δ4* may, therefore, encode for an alternative isoform of the IL-6 protein.

**In Vitro Translation of Alternatively Spliced IL-6 Isoforms**

The ability of *IL-6* mRNA isoforms to generate a protein was tested using an *in vitro* translation assay. Translation of IL-6 PCR products (containing all *IL-6* cDNA isoforms) yielded two proteins of ~ 17 and 26 kD, corresponding to a novel IL-6 splice variant and the native IL-6 protein, respectively (Figure 3A). As predicted by sequence analysis, no translation products could be detected when *IL-6Δ2* or *IL-6Δ2,4* were used as template. Con-

versely, purified *IL-6Δ4* was translated into a 17-kD protein. To select an anti-IL-6 antibody which is capable of recognizing both IL-6 isoforms we first exposed the membrane with the <sup>35</sup>S-labeled immunoprecipitates to a PhosphorImager analyzer and then used the same membrane for immunostaining with anti-IL-6 antibodies (Figure 3B).

**Expression of IL-6 Isoforms**

To prove the natural occurrence of the postulated two IL-6 isoforms, which had been obtained by *in vitro* translation, we performed immunoprecipitation using an anti-IL-6 antibody with either cell culture medium or cell lysate. As depicted in Figure 4A.1 (<sup>35</sup>S), immunoprecipitation of cell

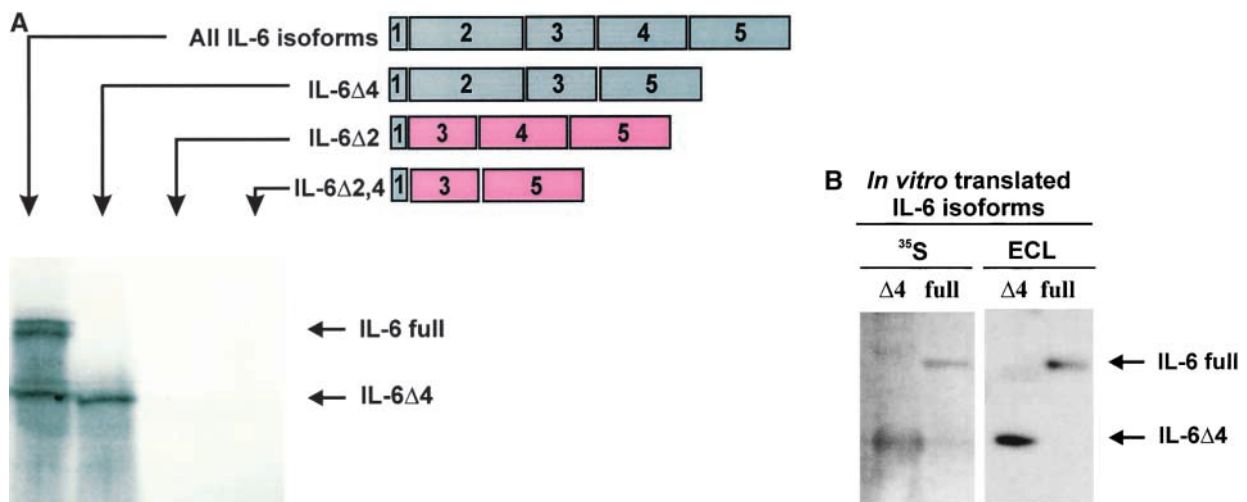


**Figure 3.** *In vitro* translation assays of IL-6 splice variants. (A) *In vitro* translation products were analyzed on a 12% denaturing polyacrylamide gel. IL-6 PCR products containing all IL-6 amplicons were translated into 26- and 17-kD proteins. *In vitro* translation of purified *IL-6Δ4* results in the expression of a single 17-kD band corresponding to the expected size of the splice variant of IL-6. In contrast, no products could be detected following translation of *IL-6Δ2* and *IL-6Δ2,4*. (B) Identification of an anti-IL-6 antibody recognizing both IL-6 protein isoforms. The panel indicated with “<sup>35</sup>S” shows the *in vitro* translated IL-6 isoforms (full-length and *IL-6Δ4*). The panel indicated with “ECL” depicts the Western blot analysis using the same membrane shown in panel “<sup>35</sup>S,” using an anti-IL-6 antibody that was capable of detecting the two isoforms of IL-6 (full-length and *IL-6Δ4*; R&D Systems, Cat. # AF-206-NA, Lot CN027041).

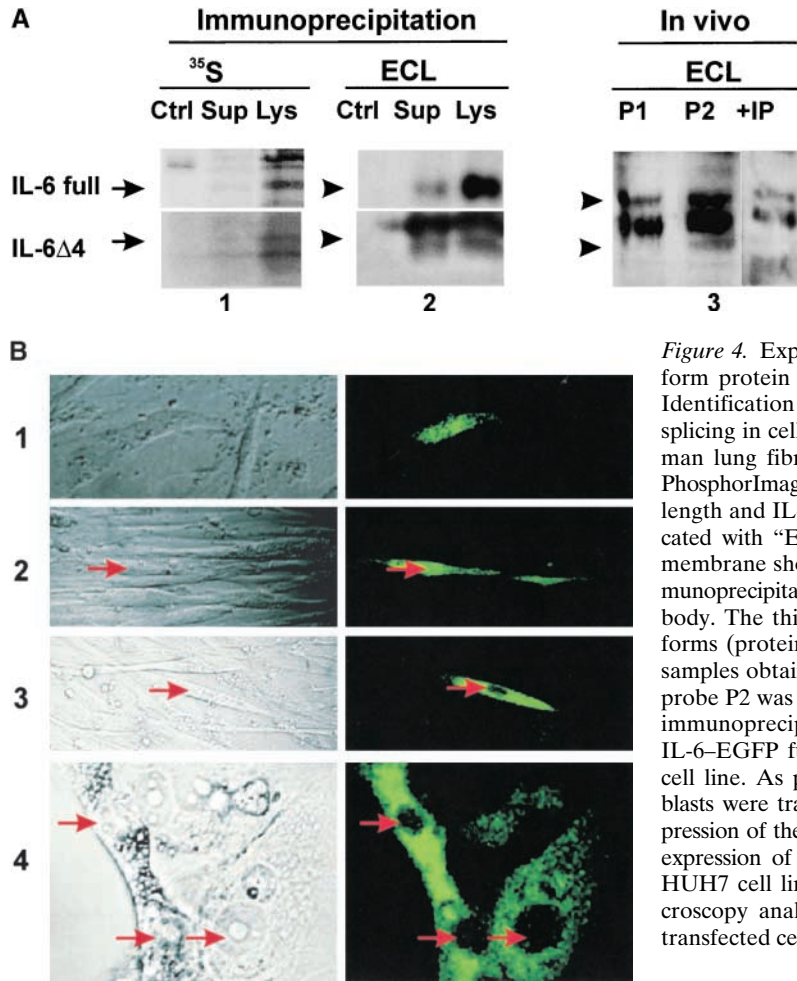


**Figure 4.** Expression of IL-6 isoforms. (A) Analysis of the IL-6 isoform protein expression in human lung fibroblast and lung tissue. Identification of the two IL-6 proteins resulting from alternative splicing in cell culture medium (Sup) and in cell lysates (Lys) of human lung fibroblasts. The panel indicated with “<sup>35</sup>S,” shows the PhosphorImager analysis of immunoprecipitated IL-6 isoforms (full-length and IL-6Δ4) in fibroblast cell cultures. The second panel indicated with “ECL” depicts the Western blot analysis using the same membrane shown in panel “<sup>35</sup>S.” “Ctrl” indicates the analysis of immunoprecipitates performed in the absence of the first anti-IL-6 antibody. The third panel demonstrates the presence of both IL-6 isoforms (protein) in the human lung. P1 and P2 represent two tissue samples obtained from different explanted lungs. +IP indicates that probe P2 was pretreated with an anti-IL-6 antibody and followed by immunoprecipitation before Western blotting. (B) Expression of IL-6-EGFP fusion protein in primary lung cells and in the HUH7 cell line. As positive control of the transfection, human lung fibroblasts were transiently transfected with the pd2EGFP vector (1). Expression of the IL-6-EGFP protein is depicted in 2. 3 and 4 depict the expression of IL-6Δ4 in transiently transfected lung fibroblasts and HUH7 cell line, respectively. *Left panels* correspond to a light microscopy analysis, *right panels* to a fluorescence analysis of these transfected cells. *Red arrows* indicate nuclei of the cells.

culture medium and cells grown in the presence of <sup>35</sup>S methionine revealed two protein bands corresponding to the molecular size of full-length IL-6 and IL-6Δ4, respectively (Figure 4A.1, <sup>35</sup>S). To confirm the identity of these IL-6 bands the membranes containing the <sup>35</sup>S-labeled proteins were used for subsequent Western blotting (Figure 4.2, ECL). Unfortunately, the band of the smaller IL-6Δ4 isoform was running close to the unspecific band originating from the light IgG chain of the monoclonal anti-IL-6 antibody used for immunoprecipitation.

Using a freshly resected lung tissue sample for Western blotting, we could show that both the full-length and IL-6Δ4 are expressed in the healthy lung; however, the ratio of IL-6 isoforms varied in the different tissue samples (Figure 4 A.3). When samples were preincubated for 1 h in the presence of neutralizing anti-IL-6 antibody, the band for full-length and IL-6Δ4 proteins disappeared, thus demonstrating the specificity of Western blot bands. (Figure 4 A.3).

In addition, we verified the expression of IL-6 isoforms in transiently transfected primary human lung fibroblasts and stably transfected HUH7 cells. Expression of the fusion protein IL-6Δ4-EGFP was detected by green fluorescence analysis (Figure 4B). IL-6Δ4 expression was found to be exclusively cytoplasmic. In contrast, the fluorescence in cells stably transfected with pd2EGFP alone or pd2EGFP-IL-6 was found to be both cytoplasmic and nuclear. This pat-

tern of expression of the IL-6 isoforms was found to be identical in lung fibroblasts and HUH7 cells in spite of the difference in the type of transfection.

To explore the structural properties of IL-6Δ4, we compared its secondary structure to that of native IL-6 and performed a three-dimensional structure analysis of IL-6Δ4.

#### Structural Comparisons of Native IL-6 and IL-6Δ4 Protein

The crystal structure of full-length IL-6 protein was shown by Xu and coworkers (25) and Somers and colleagues (26). The nucleotide sequence of exon 4 encodes for α-helices B and C corresponding to the amino acids (AAs) comprised between E81 and A131 (Figure 5). These helices are situated between two long loops joining α-helices A/A' to B and C to D/D', respectively. Interestingly, the N-terminal and C-terminal AAs of exon 4 are located in the same region in the native protein (Figure 5).

Based on an IL-6 crystal structure (PDB entry code: 2IL6), we constructed the putative structure of IL-6Δ4, omitting the AAs encoded by exon 4 using the computer program SwissPDB Viewer (Figure 5). The distance between E81 and A131 being 10.9 Å and the structural mobility of the long loops suggest that the spatial configuration of IL-6Δ4 closely resembles the one of full-length IL-6. Thus, it can be assumed that the general structural properties of IL-6 are maintained in IL-6Δ4.

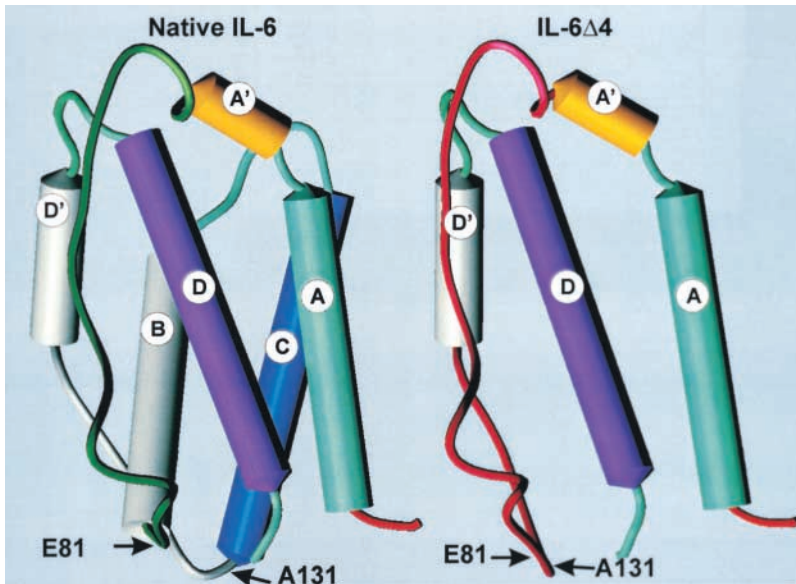


Figure 5. Computed three-dimensional structure of IL-6 $\Delta$ 4 compared with native IL-6. The two amino acids, E81 (green arm) and A131 (gray arm), in native IL-6 are joined in IL-6 $\Delta$ 4, leading to the formation of a single long loop (red arm).

Consequently,  $\alpha$ -helices A and D are joined directly in IL-6 $\Delta$ 4 and the protein structure of both IL-6 isoforms is likely to exhibit the same spatial configuration. Thus, we investigated IL-6 $\Delta$ 4 for the presence or absence of AAs known to be important in IL-6 signaling (26). As depicted in Figure 6, E106 and R113 involved in IL-6/IL-6 interaction, as well as S118/V121 required for IL-6/IL-6R $\beta$  interaction (27), are lost. On the contrary, the four AAs F74, Q175, R179, and R182, responsible for IL-6/IL-6R $\alpha$  interaction, are preserved. Therefore, IL-6 $\Delta$ 4 may be able to recognize and bind to IL-6R $\alpha$ , but may be incapable of transducing a cellular signal via the IL-6 receptor complex.

#### Binding of the IL-6 $\Delta$ 4 Protein to IL-6R $\alpha$

The role of IL-6 $\Delta$ 4 protein as a ligand to the endogenous IL-6 receptor was tested by a receptor mobility shift assay. IL-6 $\Delta$ 4 and full-length IL-6 protein were incubated with

IL-6R $\alpha$  and/or IL-6R $\beta$ , respectively, and loaded on a non-denaturing PAGE. The complexes were detected by immunoblotting against IL-6R $\alpha$  (Figure 7). Figure 6A depicts the migration of various combinations of both recombinant IL-6 receptors and recombinant full-length IL-6. Full-length IL-6 strikingly modified the migration of IL-6R $\alpha$ , especially when both IL-6 receptors were present (Figure 7A, lanes 3 and 4). Figure 7B analyzed the binding capacity of IL-6 $\Delta$ 4 to IL-6R $\alpha$ . IL-6 $\Delta$ 4 *in vitro* translated proteins were incubated with recombinant IL-6 receptors. Similar to full-length IL-6, addition of IL-6 $\Delta$ 4 resulted in a mobility shift of IL-6R $\alpha$ . In contrast to IL-6/IL-6R $\alpha$  complex, addition of IL-6R $\beta$  did not significantly affect the migration pattern of the IL-6 $\Delta$ 4/IL-6R $\alpha$  complex (Figure 7B, lane 8). No differences in migration of IL-6R $\alpha$  were detected in the presence of IL-6R $\beta$  (Figure 7B, lane 11). The unspecific signals in lanes 6 to 9 (Figure 7B) were due to

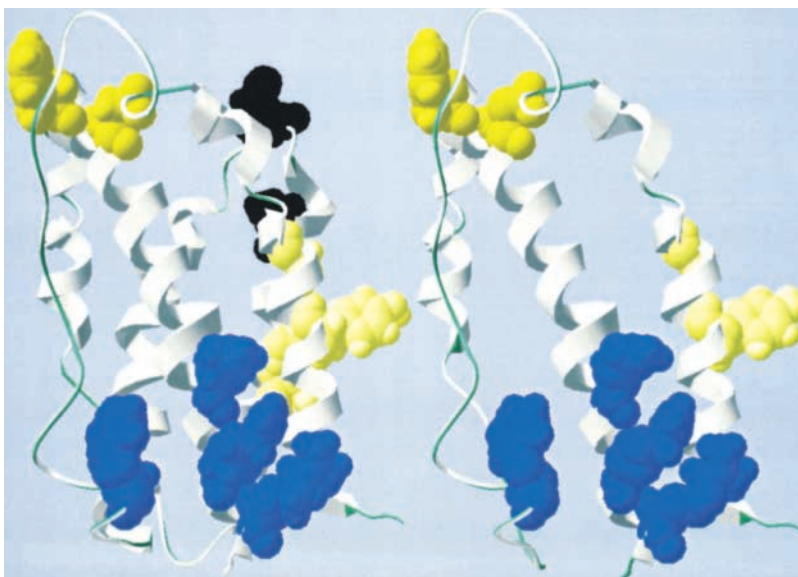
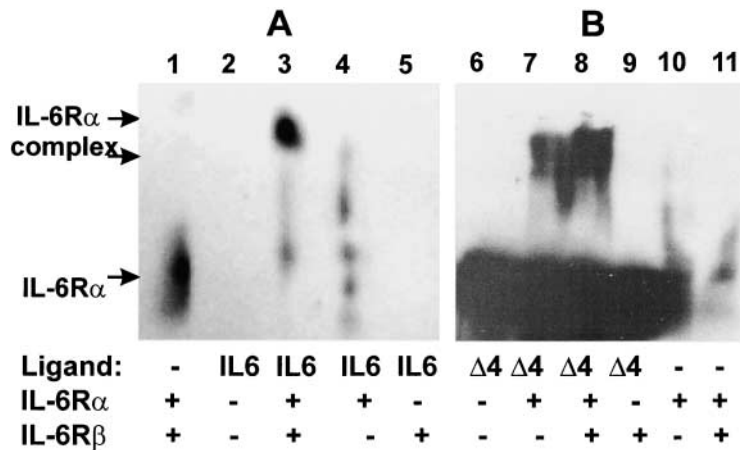


Figure 6. Description of amino acids reported to be important for IL-6 receptor complex formation in native IL-6 and compared with IL-6 $\Delta$ 4. The four amino acid residues (F75, Q176, R180, and R183) involved in the binding of IL-6 to IL-6R $\alpha$  are depicted in blue. Amino acid residues (Y32, G36, S119, V122, T158, and D161) responsible for interaction with IL-6R $\beta$  are colored in light and dark yellow, respectively. Black residues (E107 and R114) mediate IL-6/IL-6 interaction. Two (S119, V122) of the four amino acids in light yellow and both of the black residues are missing in IL-6 $\Delta$ 4.



**Figure 7.** Binding of IL-6 (A) and IL-6 $\Delta$ 4 (B) to IL-6 receptors. All receptor mobility shift experiments were evaluated by electrophoresis under nonreducing conditions and detected using an IL-6R $\alpha$  antibody. (A) Migration patterns of recombinant IL-6R $\alpha$  in combination with IL-6R $\beta$  is represented in lane 1. A receptor mobility shift of IL-6R $\alpha$  by addition of full-length IL-6 is seen in lane 4. A supershift was observed after addition of IL-6R $\beta$  to IL-6/IL-6R $\alpha$  (lane 3). (B) Migration patterns of recombinant IL-6R $\alpha$  alone or in combination with IL-6R $\beta$  is represented in lanes 10 and 11, respectively. Incubation of IL-6 $\Delta$ 4 ( $\Delta$ 4) with IL-6R $\alpha$  alone or in the presence of IL-6R $\beta$  is depicted in lanes 7 and 8, respectively. No specific band could be detected in lanes 6 and 9.

antibody crossreactivity with reticulocyte lysate proteins used in the *in vitro* translation assay as verified by Poncau's staining (data not shown).

## Discussion

In the present study we report three new *IL-6* splice variants, *IL-6 $\Delta$ 2*, *IL-6 $\Delta$ 2,4*, and *IL-6 $\Delta$ 4*, isolated from human lung tissue. *In vitro* translation of *IL-6 $\Delta$ 2* and *IL-6 $\Delta$ 2,4* yielded no detectable protein due to a shift in the reading frame leading to premature stop codons. *IL-6 $\Delta$ 4* was translated *in vitro* into a 17-kD protein, which was subsequently shown to bind to IL-6R $\alpha$ . The natural occurrence of IL-6 $\Delta$ 4 was established in fibroblast cultures by immunoprecipitation and its expression and cellular localization as a fluorescent fusion protein was established. Structural comparisons with native IL-6 suggest that the global structure of IL-6 is maintained in IL-6 $\Delta$ 4, but that AAs crucial for the formation of a functional IL-6/IL-6R $\beta$  complex are missing. Thus, IL-6 $\Delta$ 4 may have a regulatory influence on IL-6 signaling.

Analyzing IL-6 mRNAs, we detected *in vivo* as well as *in vitro* the four different mRNA isoforms resulting from alternative splicing. We were able to detect the IL-6 $\Delta$ 4 protein in cultures of human lung fibroblasts as well as in freshly isolated human lung tissue. The relative low expression of the IL-6 $\Delta$ 4 isoform corresponded with a low mRNA expression seen in RT-PCR. However, cloning of IL-6 $\Delta$ 4 sequence into the pd2EGFP vector further demonstrated its translation in living cells and strongly suggests IL-6 $\Delta$ 4 protein to be cytoplasmic. Future experiments have to clarify whether the ratio of normal IL-6 to IL-6 $\Delta$ 4 can be modified by different growth factors or by the stage of cell differentiation.

In earlier studies we characterized the role of IL-6 in the control of cell proliferation of primary human mesenchymal cells or lung tumor cell lines (28). In addition, we provided evidence for its role in hypoxia and enhanced cell proliferation in human lung cells (29). IL-6 exerts different biologic functions, regulating proliferation of mesenchymal cells via an intracellular pathway, and modulating the immune response when secreted. We investigated whether the different functions of IL-6 might be linked to alterna-

tively spliced isoforms. Based on the structural homology of the four  $\alpha$ -helices A/B and C/D, which run parallel to one another and are connected by long overhand loops, we assumed a similar regulatory mechanism for the three interleukins IL-2, IL-4, and IL-6 (7, 8, 30). A specific regulatory mechanism regulating the action of IL-2 and IL-4 has recently been described. Both genes produce alternatively spliced transcripts encoding for proteins having antagonistic properties to IL-4 (22, 31) or acting as competitive antagonists in the case of IL-2 (21, 32). It has recently been shown that the expression of an alternatively spliced isoform of IL-4 (IL-4 $\Delta$ 2), dramatically decreased in patients with asthma, indicating the important role of splice variants in biologic systems (33). Therefore, we analyzed the role of IL-6 $\Delta$ 4 protein as a possible ligand to IL-6R $\alpha$ .

The AA sequences of IL-6 $\Delta$ 4 and native IL-6 are identical with the exception of the 49 AAs encoded by exon 4 missing in IL-6 $\Delta$ 4. Although helices B and C are absent, the secondary structure ( $\alpha$ -helix) is likely to be kept in IL-6 $\Delta$ 4. Two long arms connect the two remaining  $\alpha$ -helices, A and D, also present in native IL-6, where they are located close to each other by a distance of  $\sim 10.9$  Å. In IL-6 $\Delta$ 4, AAs E81 and A131, which correspond to the C-terminal part of the first and the N-terminal part of the second arm, are directly joined together. Due to the mobility of these joined arms, the three-dimensional structure of IL-6 $\Delta$ 4 is likely to be maintained. This predicted structural homology led us to further investigate the functional properties of this splice variant at the level of ligand/receptor interaction.

Previous studies on IL-6 have demonstrated that the contact surface between IL-6 and IL-6R $\alpha$  is formed by three residues in the D helix and 1 in the A/B loop (34). In the IL-6 $\Delta$ 4 protein, these residues are conserved, suggesting a similar recognition site of IL-6 $\Delta$ 4 for IL-6R $\alpha$  as described for full-length IL-6. This was confirmed in mobility shift experiments demonstrating a strong interaction of IL-6 $\Delta$ 4 with IL-6R $\alpha$ . Addition of IL-6R $\beta$  to the IL-6 $\Delta$ 4/IL-6R $\alpha$  complex, however, did not significantly change the migration pattern of IL-6R $\alpha$ , suggesting a loss of the interaction of IL-6 $\Delta$ 4/IL-6R $\alpha$  with IL-6R $\beta$ . The same experiments with full-length IL-6 demonstrated a supershift of IL-6/IL-6R $\alpha$  complex due to the addition of IL-6R $\beta$ , illustrating the transition of a low IL-6/IL-6R $\alpha$  into a high-

## regulation of IL-6 action through alternative splicing

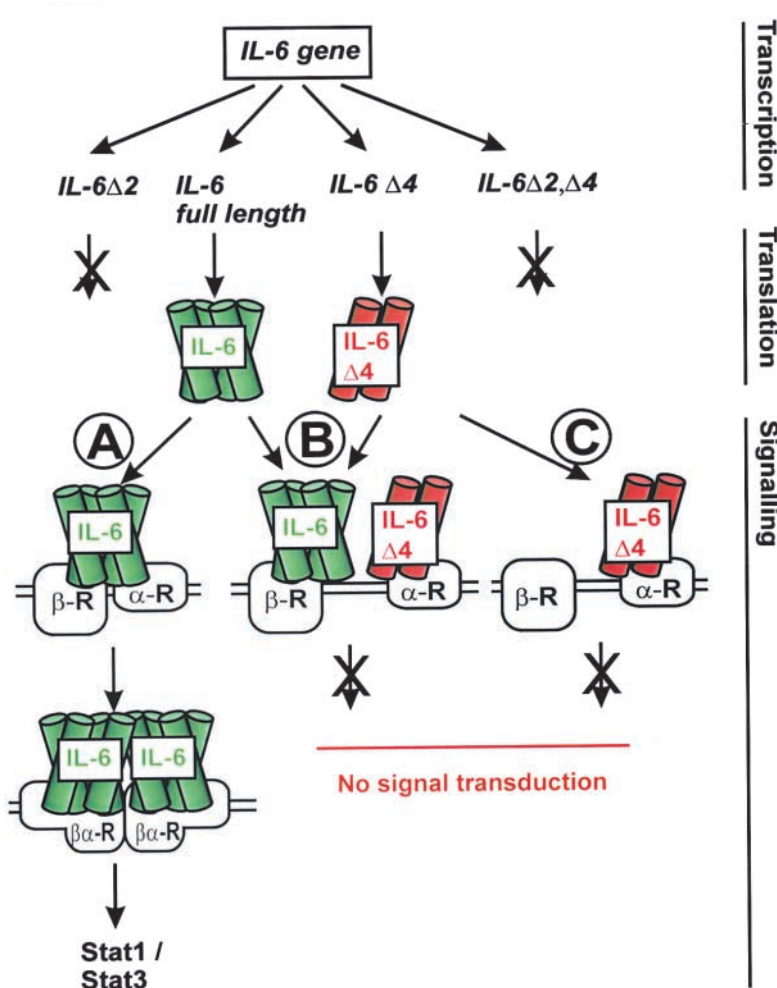


*Figure 8.* Hypothetical scheme of IL-6 isoform expression and function. The IL-6 gene is transcribed into four different IL-6 mRNA isoforms, the full-length IL-6, and three different splice variants missing exon 2 (IL-6 $\Delta$ 2), exon 4 (IL-6 $\Delta$ 4), or exon 2 and exon 4 (IL-6 $\Delta$ 2,4). Due to their respective receptor-binding properties three different binding combinations are conceivable: (i) the classic pathway, in which IL-6 binds to the IL-6R $\alpha$  and IL-6R $\beta$  forming the high affinity hexameric IL-6-receptor complex; (ii) IL-6 $\Delta$ 4 competes with full-length IL-6 for binding to the IL-6R $\alpha$  and prevents formation of the hexameric complex; or (iii) IL-6 $\Delta$ 4 binds to IL-6R $\alpha$  but fails to bind IL-6R $\beta$ .

affinity IL-6/IL-6R $\alpha$ /IL-6R $\beta$  complex. In summary, these results show that the capacity of IL-6 $\Delta$ 4 to bind to IL-6R $\alpha$  is kept and the mobility of IL-6/IL-6R $\alpha$  complex is not affected by addition of IL-6R $\beta$ .

IL-6 signaling is mediated by formation of a heterohexameric complex containing IL-6, IL-6R $\alpha$ , and IL-6R $\beta$  (2:2:2) molecules. Formation of such a complex by IL-6 $\Delta$ 4 is less likely because AAs essential for its binding to IL-6R $\beta$  (S119 and V122) are not conserved. This is in line with our observation that no significant differences in the migration pattern of the IL-6 $\Delta$ 4/IL-6R $\alpha$  complex occurred following the addition of IL-6R $\beta$ . Because IL-6 $\Delta$ 4 is missing helices B and C, the crosstalk with IL-6R $\beta$  is likely to be abolished without impeding its binding to IL-6R $\alpha$ . In addition, direct interaction between two native IL-6 proteins has been described in the functional IL-6-receptor complex. This interaction is mediated through AAs S119 and V122, which are both missing in IL-6 $\Delta$ 4. Therefore, the formation of a functional IL-6-receptor complex as a heterohexamer is likely to be impeded and argues in favor of a loss of signaling activity of IL-6 $\Delta$ 4.

A hypothetical scheme of IL-6 isoform expression and function is shown in Figure 8. Regarding their receptor binding properties, we suggest three variants of signaling depending on the IL-6 receptors complex formation: (i) the classic pathway, by which the full-length IL-6 binds to the IL-6R $\alpha$  and subsequently to the signaling receptor gp130 (IL-6R $\beta$ ), finally forming a functional hexameric complex described above (33); (ii) based on our results IL-6 $\Delta$ 4 competes with full-length IL-6 for binding to the IL-6R $\alpha$ . We hypothesize that IL-6 $\Delta$ 4/IL-6R $\alpha$  heterodimer cannot complex with high-affinity to the IL-6 full-length/IL-6R $\alpha$ /IL-6R $\beta$  heterotrimer and, therefore, signaling of IL-6 receptor complex is not possible; (iii) IL-6 $\Delta$ 4 binds to IL-6R $\alpha$ , but is unable to bind to the IL-6R $\beta$  and therefore inhibiting directly and competitively the IL-6 signaling.

In summary, we report a novel, alternatively spliced IL-6 protein isoform, IL-6 $\Delta$ 4, which lacks helices B and C, but is predicted to share structural homology with native IL-6. Considering that in IL-6 $\Delta$ 4, the AAs essential for binding to IL-6R $\alpha$  are preserved, whereas those crucial for IL-6R $\beta$  binding and IL-6/IL-6 interaction are missing, we

suggest IL-6 $\Delta$ 4 to be a competitive antagonist to native IL-6. In view of the pivotal role of IL-6 in cell growth control and cell differentiation, understanding the precise role of IL-6 $\Delta$ 4 in signal transduction will be a major issue in the biology of IL-6.

*Acknowledgments:* This work was supported by the Krebsliga beider Basel 4-98. The authors are indebted to Dr. Jean Louis Boulay and Dr. Suzana Dobie for helpful discussion of our results and this manuscript.

## References

- Akira, S., T. Taga, and T. Kishimoto. 1993. Interleukin-6 in biology and medicine. *Adv. Immunol.* 54:1-78.
- Gaillard, J. P., J. Liautard, B. Klein, and J. Brochier. 1997. Major role of the soluble interleukin-6/interleukin-6 receptor complex for the proliferation of interleukin-6-dependent human myeloma cell lines. *Eur. J. Immunol.* 27:3332-3340.
- Grafte-Faure, S., C. Leveque, M. Vasse, C. Soria, and J. P. Vannier. 1999. Recruitment of primitive peripheral blood cells: synergism of interleukin 12 with interleukin 6 and stem cell factor. *Br. J. Haematol.* 105:33-39.
- Sawamura, D., X. Meng, S. Ina, M. Sato, K. Tamai, K. Hanada, and I. Hashimoto. 1998. Induction of keratinocyte proliferation and lymphocytic infiltration by in vivo introduction of the IL-6 gene into keratinocytes and possibility of keratinocyte gene therapy for inflammatory skin diseases using IL-6 mutant genes. *J. Immunol.* 161:5633-5639.
- Florenes, V. A., C. Lu, N. Bhattacharya, J. Rak, C. Sheehan, J. M. Slingerland, and R. S. Kerbel. 1999. Interleukin-6 dependent induction of the cyclin dependent kinase inhibitor p21WAF1/CIP1 is lost during progression of human malignant melanoma. *Oncogene* 18:1023-1032.
- Fontaine, V., M. Mahieu, and J. Content. 1998. Interferon-gamma and interleukin-6 inhibit proliferation in human melanoma cells by different signalling pathways. *Melanoma Res.* 8:24-30.
- Bihl, M., M. Tamm, M. Nauck, H. Wieland, A. P. Perruchoud, and M. Roth. 1998. Proliferation of human non-small cell lung cancer cell lines: role of interleukin-6. *Am. J. Respir. Cell Mol. Biol.* 19:606-612.
- Roth, M., M. Nauck, M. Tamm, A. P. Perruchoud, R. Ziesche, and L. H. Block. 1995. Intracellular interleukin 6 mediates platelet-derived growth factor-induced proliferation of nontransformed cells. *Proc. Natl. Acad. Sci. USA* 92:1312-1316.
- Nakano, T., A. P. Chahinian, M. Shinjo, A. Tonomura, M. Miyake, N. Togawa, K. Ninomiya, and K. Higashino. 1998. Interleukin 6 and its relationship to clinical parameters in patients with malignant pleural mesothelioma. *Br. J. Cancer* 77:907-912.
- Goswami, S., A. Gupta, and S. K. Sharma. 1998. Interleukin-6-mediated autocrine growth promotion in human glioblastoma multiforme cell line U87MG. *J. Neurochem.* 71:1837-1845.
- Foti, E., G. Ferrandina, R. Martucci, M. E. Romanini, P. P. Benedetti, U. Testa, S. Mancuso, and G. Scambia. 1999. IL-6, M-CSF and IAP cytokines in ovarian cancer: simultaneous assessment of serum levels. *Oncology* 57:211-215.
- Adler, H. L., M. A. McCurdy, M. W. Kattan, T. L. Timme, P. T. Scardino, and T. C. Thompson. 1999. Elevated levels of circulating interleukin-6 and transforming growth factor-beta1 in patients with metastatic prostatic carcinoma. *J. Urol.* 161:182-187.
- Mullberg, J., E. Dittlich, L. Graeve, C. Gerhartz, K. Yasukawa, T. Taga, T. Kishimoto, P. C. Heinrich, and S. Rose-John. 1993. Differential shedding of the two subunits of the interleukin-6 receptor. *FEBS Lett.* 332:174-178.
- Mullberg, J., H. Schooltink, T. Stoyan, M. Gunther, L. Graeve, G. Buse, A. Mackiewicz, P. C. Heinrich, and S. Rose-John. 1993. The soluble interleukin-6 receptor is generated by shedding. *Eur. J. Immunol.* 23:473-480.
- Lust, J. A., K. A. Donovan, M. P. Kline, P. R. Greipp, R. A. Kyle, and N. J. Maithe. 1992. Isolation of an mRNA encoding a soluble form of the human interleukin-6 receptor. *Cytokine* 4:96-100.
- Jostock, T., G. Blinn, C. Renné, K. J. Kallen, S. Rose-John, and J. Müllberg. 1999. Immunoadhesins of interleukin-6 and the IL-6/soluble IL-6R fusion protein hyper-IL-6. *J. Immunol. Methods* 223:171-183.
- Liu, J., B. Modrell, A. Aruffo, J. S. Marken, T. Taga, K. Yasukawa, M. Murakami, T. Kishimoto, and M. Shoyab. 1992. Interleukin-6 signal transducer gp130 mediates oncostatin M signaling. *J. Biol. Chem.* 267:16763-16766.
- Taga, T., M. Narazaki, K. Yasukawa, T. Saito, D. Miki, M. Hamaguchi, S. Davis, M. Shoyab, G. D. Yancopoulos, and T. Kishimoto. 1992. Functional inhibition of hematopoietic and neurotrophic cytokines by blocking the interleukin 6 signal transducer gp130. *Proc. Natl. Acad. Sci. USA* 89:10998-11001.
- Nicholson, S. E., T. A. Willson, A. Farley, R. Starr, J. G. Zhang, M. Baca, W. S. Alexander, D. Metcalf, D. J. Hilton, and N. A. Nicola. 1999. Mutational analyses of the SOCS proteins suggest a dual domain requirement but distinct mechanisms for inhibition of LIF and IL-6 signal transduction. *EMBO J.* 18:375-385.
- Ketzinel, M., and R. Kaempfer. 1999. Cell-mediated suppression of human interleukin-2 gene expression at splicing of mRNA. *Immunol. Lett.* 68:161-166.
- Denesyuk, A. I., V. P. Zav'yalov, K. A. Denessiouk, and T. Korpela. 1998. Molecular models of two competitive inhibitors, IL-2delta2 and IL-2delta3, generated by alternative splicing of human interleukin-2. *Immunol. Lett.* 60:61-66.
- Zav'yalov, V. P., A. I. Denesyuk, B. White, V. V. Yurovsky, S. P. Atamas, and T. Korpela. 1997. Molecular model of an alternative splice variant of human IL-4, IL-4 delta 2, a naturally occurring inhibitor of IL-4-stimulated T cell proliferation. *Immunol. Lett.* 58:149-152.
- Atamas, S. P., J. Choi, V. V. Yurovsky, and B. White. 1996. An alternative splice variant of human IL-4, IL-4 delta 2, inhibits IL-4-stimulated T cell proliferation. *J. Immunol.* 156:435-441.
- Roth, M., M. Soler, M. Hornung, L. R. Emmons, P. Stulz, and A. P. Perruchoud. 1992. Cell cultures from cryopreserved human lung tissue. *Tissue Cell* 24:455-459.
- Xu, G. Y., H. A. Yu, J. Hong, M. Stahl, T. McDonagh, L. E. Kay, and D. A. Cumming. 1997. Solution structure of recombinant human interleukin-6. *J. Mol. Biol.* 268:468-481.
- Somers, W., M. Stahl, and J. S. Seehra. 1997. 1.9 A crystal structure of interleukin 6: implications for a novel mode of receptor dimerization and signaling. *EMBO J.* 16:989-997.
- Paonessa, G., R. Graziani, A. De Serio, R. Savino, L. Ciapponi, A. Lahm, A. L. Salvati, C. Toniatti, and G. Ciliberto. 1995. Two distinct and independent sites on IL-6 trigger gp 130 dimer formation and signalling. *EMBO J.* 14:1942-1951.
- Roth, M., M. Nauck, S. Yousefi, M. Tamm, K. Blaser, A. P. Perruchoud, and H. U. Simon. 1996. Platelet-activating factor exerts mitogenic activity and stimulates expression of interleukin 6 and interleukin 8 in human lung fibroblasts via binding to its functional receptor. *J. Exp. Med.* 184:191-201.
- Tamm, M., M. Bihl, O. Eickelberg, P. Stulz, A. P. Perruchoud, and M. Roth. 1998. Hypoxia-induced interleukin-6 and interleukin-8 production is mediated by platelet-activating factor and platelet-derived growth factor in primary human lung cells. *Am. J. Respir. Cell Mol. Biol.* 19:653-661.
- Boulay, J. L., and W. E. Paul. 1992. The interleukin-4 family of lymphokines. *Curr. Opin. Immunol.* 4:294-298.
- Arinobu, Y., S. P. Atamas, T. Otsuka, H. Niuro, K. Yamaoka, H. Mitsuyasu, Y. Niho, N. Hamasaki, B. White, and K. Izuhara. 1999. Antagonistic effects of an alternative splice variant of human IL-4, IL-4delta2, on IL-4 activities in human monocytes and B cells. *Cell. Immunol.* 191:161-167.
- Tsytsikov, V. N., V. V. Yurovsky, S. P. Atamas, W. J. Alms, and B. White. 1996. Identification and characterization of two alternative splice variants of human interleukin-2. *J. Biol. Chem.* 271:23055-23060.
- Seah, G. T., P. S. Gao, J. M. Hopkin, and G. A. Rook. 2001. Interleukin-4 and its alternatively spliced variant (IL-4delta2) in patients with atopic asthma. *Am. J. Respir. Crit. Care Med.* 164:1016-1018.
- Savino, R., L. Ciapponi, A. Lahm, A. Demartis, A. Cabibbo, C. Toniatti, P. Delmastro, S. Altamura, and G. Ciliberto. 1994. Rational design of a receptor super-antagonist of human interleukin-6. *EMBO J.* 13:5863-5870.